Substitution of In for Si adatoms and exchanges between In and Si adatoms on a Si(111)-7×7 surface

H. Hibino and T. Ogino
NTT Basic Research Laboratories, Atsugi, Kanagawa 243-01, Japan
(Received 28 May 1996; revised manuscript received 30 September 1996)

Substitution of In for Si adatoms and exchanges between In and Si adatoms on a Si(111)-7×7 surface have been investigated using high-temperature (HT) scanning tunneling microscopy (STM). Indium substitution probability depends on the four different types of adatoms in the 7×7 reconstruction. Differences in the In substitution energy between different types of adatoms are estimated from the substitution probability. Adatom exchange rates obtained from sequential HT-STM images are also dependent on the combination of In and Si adatoms. Measured activation energies and prefactors for exchanges on Si(111)-7×7 are comparable to those on Si(111)-$\sqrt{3}\times\sqrt{3}$. The adatom exchange is not sensitive to the adatom symmetry. HT-STM results on the adatom exchanges on Si(111) suggest that the motion of the metal adatoms is a rate-limiting step in this process. [S0163-1829(97)02511-3]

The 7×7 reconstruction on a Si(111) surface is one of the most intensively studied reconstructions, and it has come to be well understood using the dimer-adatom-stacking fault (DAS) model proposed by Takayanagi *et al.*[1] In the DAS model, two triangular regions, one of which contains a stacking fault, are connected by dimers and the triangular regions are covered with adatoms in a local 2×2 symmetry. The DAS model consists of various kinds of structural units. Therefore, the 7×7 reconstruction has been shown to have rich behavior in terms of electronic structure, chemical reactivity, and so on.[2] For example, it has been reported that clusters of metal atoms are preferentially formed on faulted halves of the unit cell.[3]

In this work, we investigated the substitution of metal atoms for Si adatoms in the 7×7 reconstruction and exchanges between metal and Si adatoms using high-temperature (HT) scanning tunneling microscopy (STM). There are four kinds of adatoms in the 7×7 reconstruction based on whether they sit on the faulted or unfaulted half of the unit cell and whether or not they are located next to the corner holes. Hereafter, we call adatoms next to the corner hole corner (C) adatoms and others middle (M) adatoms. We label C and M adatoms on the faulted half of the unit cell FC and FM and label those on the unfaulted half of the unit cell UC and UM. Electronic structures and bond configurations are dependent on the adatom type. STM (Ref. 2) and *ab initio* calculations[4] have shown that charge is transferred from the dangling bonds on the adatoms to the dangling bonds on the rest atoms and more charge is transferred from the dangling bonds on the M adatoms than those on the C adatoms. Therefore, the M adatoms show a stronger sp^2 character than the C adatoms, which explains why the C adatoms are higher than the M adatoms.

In this paper we show that the substitution probability of In depends on the adatoms type, which means that the substitution energy of In is dependent on the adatom type. It has already been reported that In atoms occupy M adatom sites rather than C adatom sites.[5,6] However, the energy difference between In M and C adatoms has not been evaluated. We obtain the substitution probability from HT-STM images and estimate the difference in the substitution energy from the probability. We further show that the substitution probability for F adatom is a little larger than that for U adatoms. We also show that the adatom exchange rate depends on the types of exchanged adatoms. Adatoms in the 7×7 reconstruction are locally arranged in a 2×2 symmetry. We have already reported the exchanges between In and Si adatoms on a Si(111)-$\sqrt{3}\times\sqrt{3}$ surface.[7] Therefore, comparing the exchange rates on the 7×7 and $\sqrt{3}\times\sqrt{3}$ surfaces clarifies how the exchange rate depends on the adatom arrangement. This provides important information about the adatom exchange mechanism.

We used a commercial STM (JEOL 4500VT) to investigate In substitution and exchange between In and Si adatoms on a Si(111)-7×7 surface. Nominally flat Si(111) samples (As-doped, $\rho = 0.001\ \Omega$ cm) were chemically cleaned by repeated oxidation in $H_2O_2:H_2SO_4$ (1:4) and oxide removal in a HF solution. After the samples were introduced into an UHV through a load lock, they were degassed at about 500 °C for 2–10 h. The samples were cleaned by flashing at 1250 °C. About 0.01 monolayers of In was deposited on the Si(111)-7×7 surface at room temperature using a W filament. In atoms were substituted for adatoms in the 7×7 reconstruction by annealing the sample at about 500 °C. The sample was annealed by passing electric currents through it. The sample temperatures below 600 °C were measured using an infrared pyrometer with a PbS detector, whose emissivity was selected so that temperatures measured with the PbS and Si pyrometers were equal at 600 °C.

Figure 1 shows sequential STM images of the In-deposited Si(111) surface at 231 °C. The sample bias was +1.4 V. In Fig. 1 there are bright and dark adatoms. As has been already reported, In atoms substitute for Si adatoms in the 7×7 reconstruction and In adatoms appear brighter than Si adatoms in the STM images taken at positive sample bias.[5] We also confirmed that In atoms substitute for surface Si atoms from STM results showing that two-dimensional Si islands are formed after annealing the sample with In depos-

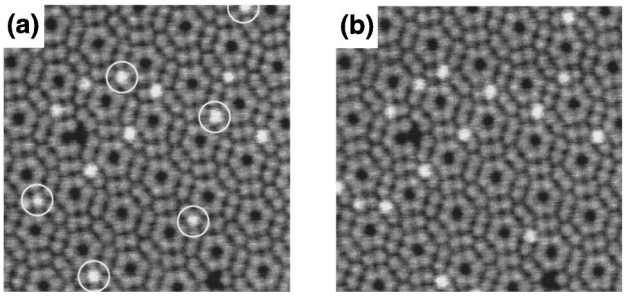

FIG. 1. Sequential HT-STM images of a Si(111) surface with 7×7 reconstruction in which In substitutes for some of the Si adatoms. It took 11 s to take the images. The measurement temperature was 231 °C. The scanning area is 14.5×14.5 nm^2. The sample bias and tunneling current were 1.4 V and 0.06 nA, respectively.

ited at room temperature. Furthermore, it has been established that, on the Al-, Ga-, and In-induced Si(111)-$\sqrt{3}\times\sqrt{3}$ surfaces, Si atoms substitute for some of the metal adatoms and metal and Si adatoms can be distinguished using STM.[8] The STM images of the regions near the boundary between the $\sqrt{3}\times\sqrt{3}$ and 7×7 domains are also consistent with the bright adatoms in the STM images at the positive sample bias being In.

Figure 1 also shows that encircled In adatoms in (a) change their positions between two images. Adatom exchange rates are obtained using such sequential HT-STM images. Here we consider only adatom exchanges in each half of the unit cell because adatom exchanges between different halves occur much less frequently than adatom exchanges in each half. There are six exchange rates corresponding to six kinds of In adatom exchange paths: from FM to FM sites, from FM to FC, from FC to FM, from UM to UM, from UM to UC, and from UC to UM. In each half of the unit cell, among $M\rightarrow M$, $M\rightarrow C$, and $C\rightarrow M$ exchange rates, $M\rightarrow M$ exchanges were the largest and $M\rightarrow C$ exchange rates were the smallest. Therefore, we first estimate the exchange rates between M adatoms. When we obtain the exchange rates from sequential STM images, we must consider the effect of multiple exchanges. Because there are only three M sits in each half, these effects are especially serious. We assume that there is an In M adatom in each half of the unit cell and the adatoms are restricted to being M adatoms. At $t=0$, the In adatom sits on one of the three M sites. The probability $p_1(t)$ of the adatom being at the initial position at a time t later and the probability $p_2(t)$ of the adatom being at one of the other two positions are obtained using the differential equations

$$dp_1/dt=-2rp_1+2rp_2, \quad dp_2/dt=rp_1-rp_2, \qquad (1)$$

where r is the exchange rate between two M adatoms. The initial conditions are $p_1(0)=1$ and $p_2(0)=0$. Then,

$$p_1(t)=\tfrac{1}{3}+\tfrac{2}{3}\exp(-3rt), \quad p_2(t)=\tfrac{1}{3}-\tfrac{1}{3}\exp(-3rt). \qquad (2)$$

To obtain the exchange rate, we first obtain the ratio p_1 of unmoving M adatoms to total M adatoms between the two STM images taken at an interval t. Then, r is estimated using Eq. (2). For $M\rightarrow C$ and $C\rightarrow M$ exchange rates, however, we

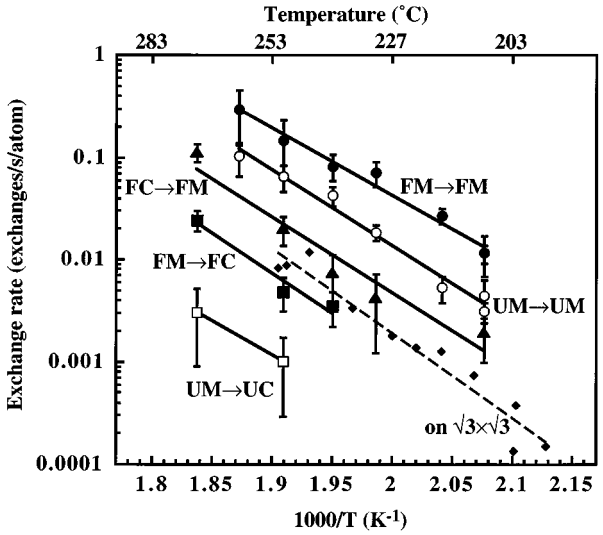

FIG. 2. Temperature dependences of exchange rates between In and Si adatoms from HT-STM images. Exchange rates on a Si(111)-$\sqrt{3}\times\sqrt{3}$ surface measured from HT-STM images at the positive sample biases are also plotted as references, but these values are $\frac{1}{6}$ of the values in Ref. 7 because the adatoms on the $\sqrt{3}\times\sqrt{3}$ surface have six nearest-neighbor adatoms.

did not consider the effects of multiple exchanges because the exchange rates were much smaller than $M\rightarrow M$ exchanges. The $M\rightarrow C$ ($C\rightarrow M$) exchange rate was obtained using the numbers of the M (C) adatoms n and the $M\rightarrow C$ ($C\rightarrow M$) exchange events n_E, which were measured from STM images, as $r=n_E/2nt$. In this equation, the 2 in the denominator of the right-hand side appears because each M (C) adatom has two nearest-neighbor C (M) adatoms.

In Fig. 2 we plot the obtained five exchange rates ($FM\rightarrow FM$, $FM\rightarrow FC$, $FC\rightarrow FM$, $UM\rightarrow UM$, and $UM\rightarrow UC$ exchanges) as a function of temperature. The HT-STM images used for obtaining the exchange rates were taken at sample biases between 1.4 and 1.9 V. The In$\leftrightarrow$Si exchange rates on Si(111)-$\sqrt{3}\times\sqrt{3}$, obtained from HT-STM images taken at the positive sample bias, are also plotted as references, but these values are $\frac{1}{6}$ of the values in Ref. 7 because adatoms on the $\sqrt{3}\times\sqrt{3}$ surface have six nearest-neighbor adatoms. We also obtained the $UC\rightarrow UM$ exchange rates, but did not plot them in Fig. 2 because they included a large statistical uncertainty due to the fact that number of the UC adatoms is the lowest among six kinds of adatoms.

Activation energies E and prefactors f are obtained for each type of the adatom exchange. For the $FM\rightarrow FM$, $FM\rightarrow FC$, $FC\rightarrow FM$, and $UM\rightarrow UM$ exchanges, E's and f's are obtained by fitting the temperature dependence of the exchange rate in an Arrhenius form $r=f\exp(-E/kT)$. For the $UM\rightarrow UC$ and $UC\rightarrow UM$ exchanges, we assume that their f's are equal to the f of the $UM\rightarrow UM$ exchange and their E's are different. The activation energies were estimated from the ratio of the $UM\rightarrow UC$ or $UC\rightarrow UM$ exchange rate to the $UM\rightarrow UM$ exchange rate. The obtained activation energies and prefactors are listed in Table I. The f's for the exchanges in the faulted half are close. This verifies the assumption on which we obtained E's for the $UM\rightarrow UC$ and $UC\rightarrow UM$ exchanges. It has been reported,

TABLE I. Prefactors and activation energies for exchanges between In and Si adatoms. Values for $\sqrt{3}\times\sqrt{3}$ surface measured at both sample positive and negative biases are also quoted from Ref. 7, but the prefactors are divided by six because the adatoms on the $\sqrt{3}\times\sqrt{3}$ surface have six nearest-neighbor adatoms. Activation energies and prefactors for the $FM\rightarrow FM$, $FM\rightarrow FC$, $FC\rightarrow FM$, and $UM\rightarrow UM$ exchanges were obtained by fitting the temperature dependence of the exchange rate in an Arrhenius form. For $UM\rightarrow UC$ and $UC\rightarrow UM$ exchanges, we assume that their prefactors are equal to the prefactor of the $UM\rightarrow UM$ exchange and their activation energies were estimated from the ratios between the exchange rates.

Surface	Exchange	E (eV)	f (s^{-1})
Si(111)-7×7	$FM\rightarrow FM$	1.31 ± 0.08	$2\times10^{12\pm0.8}$
	$FC\rightarrow FM$	1.47 ± 0.22	$7\times10^{12\pm2.2}$
	$FM\rightarrow FC$	1.52 ± 0.31	$6\times10^{12\pm3.0}$
	$UM\rightarrow UM$	1.49 ± 0.10	$2\times10^{13\pm1.0}$
	$UC\rightarrow UM$	1.60	
	$UM\rightarrow UC$	1.69	
Si(111)-$\sqrt{3}\times\sqrt{3}$	In $V_S>0$	1.56 ± 0.15	$1\times10^{13\pm1.6}$
	In $V_S<0$	1.33 ± 0.11	$1\times10^{11\pm1.1}$

based on results of perturbed $\gamma\gamma$ angular correlation, that the activation energy for the conversion from C to M adatoms is 1.61 ± 0.15 eV.[6] This value is very close to the E's for the $C\rightarrow M$ exchanges.

Next, we obtain In substitution probabilities dependent on the adatom type from HT-STM images. At the measured temperatures used to obtain the adatom exchange rates (208 °C–272 °C), adatoms are exchanged in each half of the unit cell, but not between different halves. In particular, all the exchange rates in each half of the unit cell are larger than 10^{-4} s^{-1} above 230 °C. Because we typically waited more than 1 h before starting the HT-STM measurements and 30 min after changing the sample temperature in the course of the measurement to reduce the thermal drift of the sample, the ratio of the number of C adatoms n_C to the number of M adatoms n_M in each of the faulted and unfaulted halves is equilibrated in the HT-STM images taken at 272 °C–230°C. However, in these STM images, the ratio of the number of the adatoms in the faulted half n_F to the number of the adatoms in the unfaulted half n_U is not an equilibrium value, but rather freezing of the ratio occurs at a temperature higher than 272 °C. Therefore, to estimate the freezing temperature of the In adatom exchanges between different halves of the unit cell, HT-STM images were taken at 298 °C and 307 °C. Figure 3 shows HT-STM images taken at 298 °C. It took 9 s to take each image with an 11-s interval between the end of the first scan and the start of the next. In Fig. 3 In adatoms are exchanged so frequently in each half of the unit cell that they do not usually look circular. However, we can judge in which half of the unit cell there is an adatom. In Fig. 3(a) there is an In adatom in half unit A, but there is no In adatom in half unit B. On the other hand, in Fig. 3(b), there is no In adatom in A, but there is an adatom in B. We have no direct evidence that the In adatom in A and the In adatom in B are the same atom. However, we observed the same situation as that in Figs. 3(a) and 3(b) in many other pairs of HT-STM images. Therefore, we infer that the In adatom

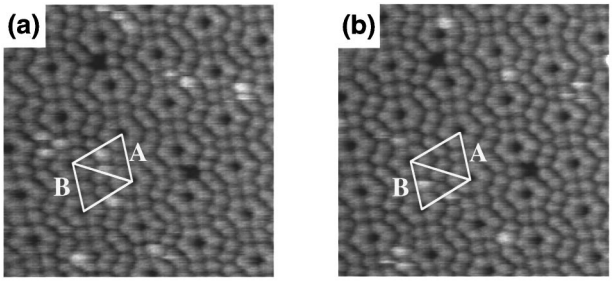

FIG. 3. HT-STM images of a Si(111) surface with 7×7 reconstruction in which In substitutes for some of the Si adatoms. It took 9 s to take the images with an 11-s interval between images. The measurement temperature was 298 °C. The scanned area was 15.5×15.5 nm^2. The sample bias and tunneling current were 1.3 V and 0.04 nA, respectively.

moved from A in image (a) to B in image (b). Furthermore, we observed the disappearance or appearance of In adatoms from one image to the next. However, cases of adatom shift to one of the nearest halves was observed more frequently than the disappearance or appearance of the adatom. Therefore, we infer that the In adatom moves to one of the nearest halves of the unit cell more frequently than it moves a long distance. The rate of the In motion across the boundary of the half of the unit cell was 1.3×10^{-3} s^{-1} at 298 °C and 2.0×10^{-3} s^{-1} at 307 °C. Assuming that the In motion across the dimer region is a thermal activated process and that the prefactor is close to that of the adatom exchange in each half of the unit cell (2×10^{12}–2×10^{13}), the activation energy is 1.72–1.84 eV. Using these values, the rate is 0.1 at about 380 °C and 1 at about 430 °C. Therefore, we conjecture that In adatom motion between the different halves of the unit cell freezes at about 400 °C.

$n_{FC}/(n_{FC}+n_{FM})$ and $n_{UC}/(n_{UC}+n_{UM})$ measured from HT-STM images at 231 °C–272 °C were both 0.14. This value is very close to the reported $n_M:n_C$ of 6:1 (Ref. 5) and 5:1.[6] Substitution of In for M adatoms is energetically more favorable than for C adatoms. The differences in the substitution energy ΔE_S are estimated from the value of $n_{FC}/(n_{FC}+n_{FM})$ and $n_{UC}/(n_{UC}+n_{UM})$ using the relation $n_C/(n_C+n_M)=1/[1+\exp(\Delta E_S/kT)]$. ΔE_S for the F and U adatoms are 82 ± 14 and 82 ± 15 meV, respectively. The measured value of $n_F/(n_F+n_U)$ was 0.57. This indicates that the In substitution for adatoms in the faulted half is energetically more favorable than in the unfaulted half. The energy difference is about 16 ± 5 meV. Here we also note that the energy difference between M and C adatoms and the difference between the activation energies for the $M\rightarrow C$ and $C\rightarrow M$ exchanges are complementary since $n_M f_{M\rightarrow C}\exp(-E_{M\rightarrow C}/kT) = n_C f_{C\rightarrow M}\exp(-E_{C\rightarrow M}/kT)$ under equilibrium. If $f_{M\rightarrow C}=f_{C\rightarrow M}$, $\Delta E_S=E_{M\rightarrow C}-E_{C\rightarrow M}$. These relations are almost satisfied for both faulted and unfaulted halves.

The question is what causes the site selectivity of In adatoms. For the energy of the adatom, the charge transfer and bond configuration are important. In each half of the unit cell, more charge is transferred to the dangling bonds on the rest atoms from the dangling bonds on the M adatoms than from the dangling bonds on the C adatoms.[2] Indium acts as

an acceptor in the bulk Si. It is, therefore, contradictory that more In atoms occupy *M* sites than *C* sites. It is difficult to explain site selectivity in terms of charge transfer between In adatoms and Si rest atoms.

We have considered two factors to explain site selectivity. One is strain relaxation by In substitution for the Si adatom. The other is hybridization of the In adatom. Although we have no data on the surface stress of In adatom structures, it has been reported that the $\sqrt{3}\times\sqrt{3}$ Ga-adatom surface is less tensilely strained than the $\sqrt{3}\times\sqrt{3}$ Si-adatom surface.[9] Because Ga contributes three electrons to the bonds with its neighbors, a Ga adatom prefers a more sp^2-like bond configuration. Therefore, the bond angles of the Ga adatom are larger than those of the Si adatom.[6] This causes the distance between the first-layer atoms bonded with the adatom to increase, resulting in decreased surface tensile stress.[9] Indium is also trivalent and *ab initio* calculations of the Al-, Ga-, and In-induced Si(111)-$\sqrt{3}\times\sqrt{3}$ surfaces have shown similar substantial substrate relaxations.[10] Therefore, the In adatom structure is probably less tensilely strained than the Si adatom structure. According to Vanderbilt's *ab initio* calculation, the faulted 2×2 adatom structure has more tensile stress than the unfaulted 2×2 structure.[11] Therefore, more energy is gained when In substitutes for *F* adatoms than *U* adatoms, which agrees with our results. However, the site selectivity of *M* adatoms being higher than that of *C* adatoms is not explained by the relaxation of the tensile stress in the adatom cell. Because an *ab initio* calculation of surface stress is beyond our power, we have simply compared the separations between first-layer atoms bonded with *M* and *C* adatoms as a measure of surface stress.[9] These separations, which were obtained using the atomic positions shown in Ref. 4, are shorter than the bulk value, which corresponds to a tensile stress in the adatom cell.[9] Furthermore, the average separation between the first-layer atoms bonded with the *C* adatom is shorter than that between the first-layer atoms bonded with the *M* adatom. This means that the *C* adatom cell has more tensile stress than the *M* adatom cell. Therefore, the energy gain due to the strain relaxation would be larger for *C* adatoms than for *M* adatoms, which contradicts the site selectivity.

The preferential substitution of In for *M* adatoms rather than for *C* adatoms is probably due to the hybridization of the In adatom. The adatom cell in the 7×7 reconstruction is connected to the dimer and the dimer bond is longer than the bulk bond,[4] which causes the compressive stress in the dimer cell. This compressive stress probably resists expansion of the separation between first-layer atoms bonded with the adatom and the dimer. We therefore suppose that relaxation of positions of Si atoms around the adatom is small when In substitutes for an Si adatom. This means the energy gain due to strain relaxation is small. In this situation, because *M* adatoms have a stronger sp^2 (weaker sp^3) character than *C* adatoms, the bond configuration of In *C* adatom is more energetically unfavorable than that of In *M* adatom. The balance between the energy gain through the strain relaxation and the energy cost due to the unfavorable bond configuration seems to explain the site selectivity well. However, *ab initio* energy and stress calculations are necessary in order to clearly understand the origin of the site selectivity.

We have also investigated exchanges between metal and Si adatoms on Si(111)-$\sqrt{3}\times\sqrt{3}$ surfaces.[7,12] The activation energies for Pb, Al, Ga, and In adatoms are between 1.2 and 1.7 eV and the prefactors are between 2×10^9 and 6×10^{13} s^{-1}.[7,12] The *E*'s and *f*'s for adatom exchanges on the 7×7 surface are comparable to those for adatom exchanges on Si(111)-$\sqrt{3}\times\sqrt{3}$. The *f*'s for these adatom exchanges are also close to the reported *f*'s for the various surfaces diffusion processes represented by the *f*'s for metal diffusion on metal surfaces obtained using field ion microscopy.[13] This means that the adatom exchanges are a singly activated process. We have shown that there are two possible singly activated processes to explain the adatom exchange.[7] One is that some atoms move cooperatively so as to provide a potential barrier. This is similar to the well-known concerted exchange mechanism for metal adatom diffusion on metal surfaces.[14] The other is a rather simple mechanism in which the motion of metal adatoms is a rate-limiting process. Adatoms in the 7×7 reconstruction are locally arranged in a 2×2 symmetry. Because the local adatom arrangement on the 7×7 surface is quite different from the $\sqrt{3}\times\sqrt{3}$ arrangement, the concerted motions for the adatom exchanges on the 7×7 and $\sqrt{3}\times\sqrt{3}$ surfaces would be totally different. However, the activation energies are rather similar. Therefore, it is reasonable to imagine that the rate-limiting process in the adatom exchange is for metal adatoms to leave stable T_4 sites and become mobile. Thus the *f*'s and *E*'s on the 7×7 and $\sqrt{3}\times\sqrt{3}$ surfaces are rather close.

In summary, we have investigated substitution of In atoms for Si adatoms and exchanges between In and Si adatoms on Si(111)-7×7 using HT-STM. We obtained substitution probabilities of In for four different adatom sites and estimated the difference in the substitution energies from the substitution probabilities. We also obtained various kinds of adatom exchange rates from sequential HT-STM images and estimated prefactors and activation energies for the adatom exchanges. These prefactors and activation energies are comparable to those for the adatom exchanges on the Si(111)-$\sqrt{3}\times\sqrt{3}$ surfaces. This indicates that the prefactors and activation energies between metal and Si adatoms on Si(111) surfaces are not sensitive to the adatom arrangement.

[1] K. Takayanagi, Y. Tanishiro, M. Takahashi, and S. Takahashi, J. Vac. Sci. Techol. A **3**, 1502 (1985).

[2] For example, R. Wolkow and Ph. Avouris, Phys. Rev. Lett. **60**, 1049 (1988).

[3] U. K. Köhler, J. E. Demuth, and R. J. Hamers, Phys. Rev. Lett. **60**, 2499 (1988); St. Tosch and H. Neddermeyer, *ibid.* **61**, 349 (1988).

[4] I. Stich, M. C. Payne, R. D. King-Smith, J.-S. Lin, and L. J. Clarke, Phys. Rev. Lett. **68**, 1351 (1992); K. D. Brommer, M. Needels, B. E. Larson, and J. D. Joannopoulos, *ibid.* **68**, 1355 (1992).

[5] J. Nogami, S.-I. Park, and C. F. Quate, J. Vac. Sci. Technol. B **6**, 1479 (1988).

[6] G. Krausch, T. Detzel, R. Fink, B. Luckscheiter, R. Platzer, U.

Wöhrmann, and G. Schatz, Phys. Rev. Lett. **68**, 377 (1992).
[7] H. Hibino and T. Ogino, Phys. Rev. B **54**, 5763 (1996).
[8] R. J. Hamers and D. E. Demuth, Phys. Rev. Lett. **60**, 2527 (1988); R. J. Hamers, Phys. Rev. B **40**, 1657 (1989); P. Bedrossian, K. Mortensen, D. M. Chen, and J. A. Golovchenko, Nucl. Instrum. Methods Phys. Res. Sect. B **48**, 296 (1990); J. Nogami, S.-I. Park, and C. F. Quate, Phys. Rev. B **36**, 6221 (1987).
[9] R. D. Meade and D. Vanderbilt, Phys. Rev. Lett. **63**, 1404 (1989).
[10] J. E. Northrup, Phys. Rev. Lett. **53**, 683 (1984); J. M. Nicholls, P. Mårtensson, G. V. Hansson, and J. E. Northrup, Phys. Rev. B **32**, 1333 (1985); J. M. Nicholls, and B. Reihl, and J. E. Northrup, *ibid.* **35**, 4137 (1987); J. Zegenhagen, J. R. Patel, P. Freeland, D. M. Chen, J. A. Golovchenko, P. Bedrossian, and J. E. Northrup, *ibid.* **39**, 1298 (1989).
[11] D. Vanderbilt, Phys. Rev. Lett. **59**, 1456 (1987).
[12] H. Hibino and T. Ogino, Surf. Sci. **328**, L547 (1995); **364**, L547 (1996).
[13] For example, T. T. Tsong, Prog. Surf. Sci. **10**, 165 (1980); Rep. Prog. Phys. **51**, 759 (1988); G. L. Kellogg, Surf. Sci. Rep. **21**, 1 (1994).
[14] G. L. Kellogg and P. J. Feibelman, Phys. Rev. Lett. **64**, 3143 (1990); C. Chen and T. T. Tsong, *ibid.* **64**, 3147 (1990); P. J. Feibelman, *ibid.* **65**, 729 (1990).